LBL-37340
UC-410

Lawrence Berkeley Laboratory
UNIVERSITY OF CALIFORNIA

Accelerator & Fusion Research Division

Presented at the Fourteenth International Conference on Magnetic Technology, Tampere, Finland, June 11–16, 1995, and to be published in the Proceedings

Three Dimensional Pure Permanent Magnet Undulator Design Theory

R.D. Schlueter and S. Marks

June 1995

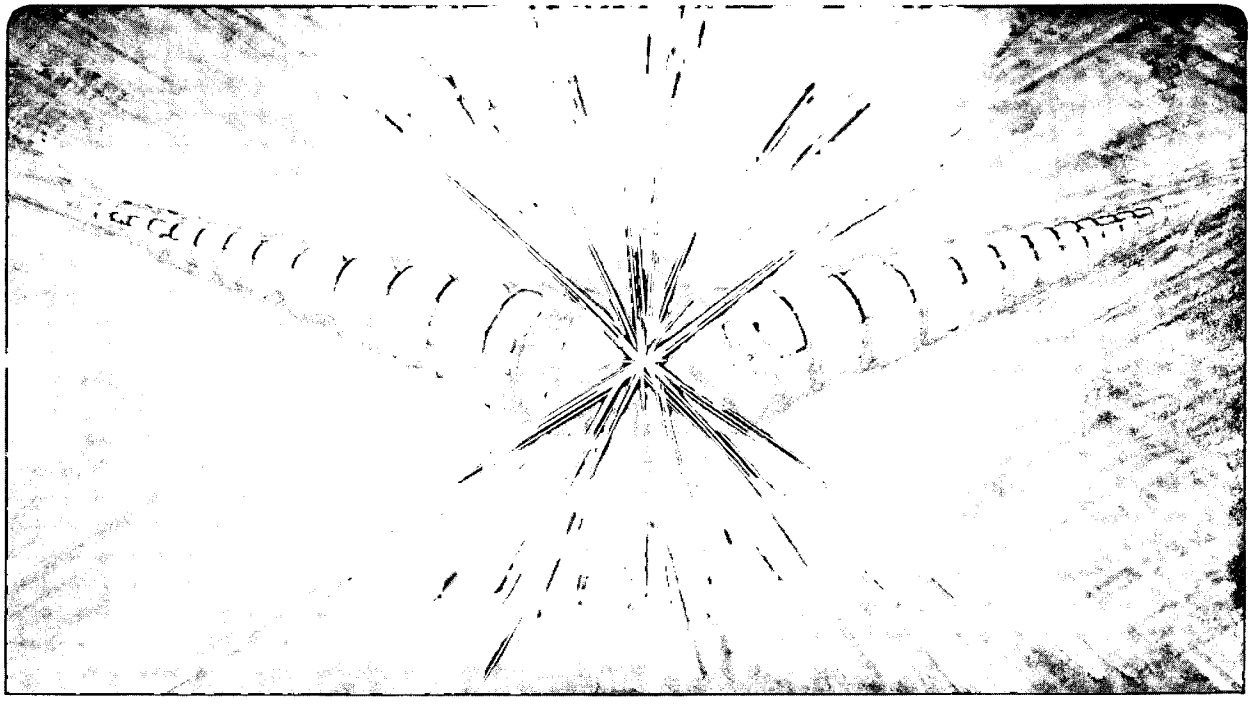

REFERENCE COPY
Does Not
Circulate
Bldg. 50 Library.
LBL-37340
Copy 1

Prepared for the U.S. Department of Energy under Contract Number DE-AC03-76SF00098

DISCLAIMER

This document was prepared as an account of work sponsored by the United States Government. While this document is believed to contain correct information, neither the United States Government nor any agency thereof, nor The Regents of the University of California, nor any of their employees, makes any warranty, express or implied, or assumes any legal responsibility for the accuracy, completeness, or usefulness of any information, apparatus, product, or process disclosed, or represents that its use would not infringe privately owned rights. Reference herein to any specific commercial product, process, or service by its trade name, trademark, manufacturer, or otherwise, does not necessarily constitute or imply its endorsement, recommendation, or favoring by the United States Government or any agency thereof, or The Regents of the University of California. The views and opinions of authors expressed herein do not necessarily state or reflect those of the United States Government or any agency thereof, or The Regents of the University of California.

Lawrence Berkeley National Laboratory
is an equal opportunity employer.

DISCLAIMER

This document was prepared as an account of work sponsored by the United States Government. While this document is believed to contain correct information, neither the United States Government nor any agency thereof, nor the Regents of the University of California, nor any of their employees, makes any warranty, express or implied, or assumes any legal responsibility for the accuracy, completeness, or usefulness of any information, apparatus, product, or process disclosed, or represents that its use would not infringe privately owned rights. Reference herein to any specific commercial product, process, or service by its trade name, trademark, manufacturer, or otherwise, does not necessarily constitute or imply its endorsement, recommendation, or favoring by the United States Government or any agency thereof, or the Regents of the University of California. The views and opinions of authors expressed herein do not necessarily state or reflect those of the United States Government or any agency thereof or the Regents of the University of California.

LBL-37340
LSGN-216
UC-410

THREE DIMENSIONAL PURE PERMANENT MAGNET UNDULATOR DESIGN THEORY*

Ross D. Schlueter and Steve Marks

Advanced Light Source
Accelerator and Fusion Research Division
Lawrence Berkeley Laboratory
University of California
Berkeley, CA 94720

June 1995

Paper presented at the 14th International Conference on Magnetic Technology,
Tampere University of Technology, Finland, June 11-16, 1995

*This work was supported by the Director, Office of Energy Research, Office of Basic Energy Sciences, Materials Sciences Division, of the U. S. Department of Energy, under Contract No. DE-AC03-76SF00098.

Three-Dimensional Pure Permanent Magnet Undulator Design Theory

R.D. Schlueter and S. Marks
Lawrence Berkeley Laboratory, Berkeley, California 94720

Abstract—**Expressions for fields due to a point charge in 3D and due to a line charge in 2D are compared. Extensions to dipoles are made with emphasis on the relationship between dipole orientation and field component magnitudes. Differences between the effects on fields of dipole rotations in 2D and in 3D are highlighted and formulas for maximizing individual field components are given. A final macrogeometry extension is made and a closed-form expression is developed to calculate the field due to an arbitrary 3D configuration of permanent magnet (PM) blocks. The field optimization theory is applied to the design of the ALS elliptically polarizing undulator (EPU). Utilizing 3D field enhancement, peak on-axis field in practical designs can be increased typically by 5% to 40% or more over their 2D counterparts. The theory is generally applicable to any pure (i.e., no soft magnetic material) PM design.**

I. Introduction

The theory of pure permanent magnet (PM) design in two dimensions has been described thoroughly [1,2]. Design of both nominally 2D pure PM structures, e.g., linearly polarizing undulators, and inherently 3D pure PM structures, e.g., Sasaki-type [3,4] planar elliptically polarizing undulators, can benefit from the extension of these concepts and optimization techniques to $\Re^3$. Herein, the PM material with $\mu = 1$ is represented by magnetic charge sheets on surfaces [5,6].

II. PM POINT CHARGES AND DIPOLES

A. Point charge.

In $\Re^3$ the scalar potential and field from a point charge q [G-cm^2] located at $\mathbf{r}_q \equiv (x_q, y_q, z_q)$ are, respectively,

$$4\pi V(\mathbf{r}) = q/|\mathbf{r}-\mathbf{r}_q|; \;\; 4\pi\mathbf{B}(\mathbf{r}) = q(\mathbf{r}-\mathbf{r}_q)/|\mathbf{r}-\mathbf{r}_q|^3, \quad (1)$$

Manuscript received June 13, 1995.
This work was supported by the Director, Office of Energy Research, Office of Basic Energy Sciences, Mat. Sci. Div., of the U.S. Dept. of Energy, Contract No. DEAC03-76SF00098.

For a line charge of strength q' [G-cm^2/cm] per unit length in z, the field is 2D and is given by

$$4\pi\mathbf{B}(\mathbf{r}) = \int_{-\infty}^{\infty} \frac{q'(\mathbf{r}-\mathbf{r}_q)}{|\mathbf{r}-\mathbf{r}_q|^3} dz = \frac{2q'(x-x_q, y-y_q)}{|\mathbf{r}-\mathbf{r}_q|^2}. \quad (2)$$

The field conjugate is an analytic function of the complex variable $t \equiv x + iy$: $B^*(t) \equiv B_x - iB_y = q'/2\pi(t - t_q)$.

B. Dipole.

Extension to a dipole, where at $\mathbf{r}_q$ point charges of strength $\pm q$ separated by l are oriented according to direction cosines $\hat{\eta}_q \equiv (\cos\chi, \cos\psi, \cos\theta)$, gives in 3D:

$$\frac{4\pi|\mathbf{r}_q - \mathbf{r}|^5}{ql} \begin{pmatrix} B_x(\mathbf{r}) \\ B_y(\mathbf{r}) \\ B_z(\mathbf{r}) \end{pmatrix} = \quad (3)$$

$$\begin{pmatrix} 2\hat{x}_q^2 - \hat{y}_q^2 - \hat{z}_q^2 & 3\hat{x}_q\hat{y}_q & 3\hat{x}_q\hat{z}_q \\ 3\hat{x}_q\hat{y}_q & 2\hat{y}_q^2 - \hat{x}_q^2 - \hat{z}_q^2 & 3\hat{y}_q\hat{z}_q \\ 3\hat{x}_q\hat{z}_q & 3\hat{y}_q\hat{z}_q & 2\hat{z}_q^2 - \hat{x}_q^2 - \hat{y}_q^2 \end{pmatrix} \begin{pmatrix} \cos\chi \\ \cos\psi \\ \cos\theta \end{pmatrix}$$

where $\hat{x}_q \equiv x_q - x$, etc. For a permanent magnet $q = \mathbf{B}_r \cdot \mathbf{a}$, where $\mathbf{B}_r$ is the remanent field and $\mathbf{a}$ is the surface normal.

For a line dipole of strength $q' = \mathbf{B}_r \cdot \mathbf{a}'$ in 2D:

$$\frac{2\pi|\hat{\mathbf{r}}_q|^4}{q'l} \begin{pmatrix} B_x(\mathbf{r}) \\ B_y(\mathbf{r}) \end{pmatrix} = \begin{pmatrix} \hat{x}_q^2 - \hat{y}_q^2 & 2\hat{x}_q\hat{y}_q \\ 2\hat{x}_q\hat{y}_q & \hat{y}_q^2 - \hat{x}_q^2 \end{pmatrix} \begin{pmatrix} \cos\chi \\ \cos\psi \end{pmatrix} \quad (4)$$

Since $\hat{\eta}_q = e^{i\chi}$, field conjugate $B^*(t) = q'le^{i\chi}/2\pi(t_q - t)^2$. Note that for a 2D line dipole oriented in, say, the x-direction, there is no B_x component at $\mathbf{r} = 0$ when that line charge is located along the line $y_q = \pm x_q$. At this location, this orientation also maximizes $B_y(0,0)$. This contrasts with the 3D case of a point dipole so oriented, which gives rise to a pure B_y component on-axis at $z = z_q$ when it lies along the line $y_q = \pm\sqrt{2}x_q$, though at this location $B_y(\mathbf{r} = 0)$ is not maximized by this orientation.

C. Easy axis rotation.

In 2D, dipole rotation by an angle $\Delta\chi$ has the effect of rotating $\mathbf{B}$ by $-\Delta\chi$, while $|B|$ remains unchanged [1]:

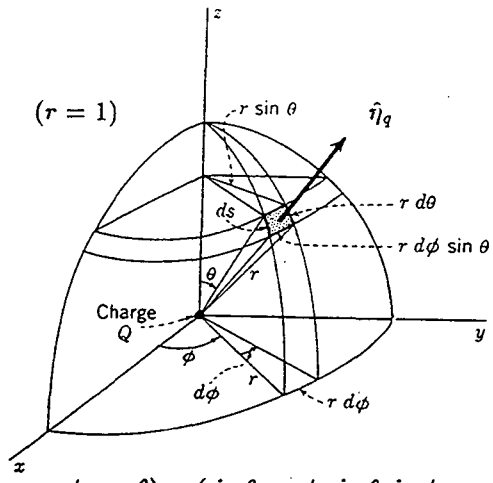

$\hat{\eta}_q \equiv (\cos\chi, \cos\psi, \cos\theta) = (\sin\theta\cos\phi, \sin\theta\sin\phi, \cos\theta)$

Fig. 1. Direction cosines of dipole at $\mathbf{r}_q = 0$

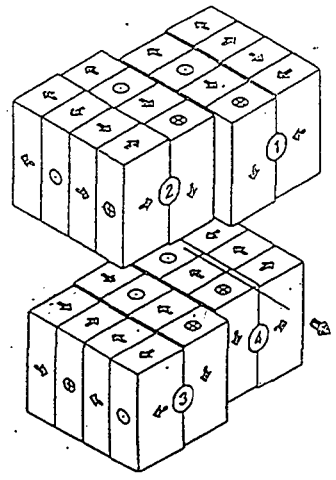

Fig. 2. ALS EPU periodic structure

$$B_2^* = \frac{q' l e^{i(\chi+\Delta\chi)}}{2\pi(t_q - t)^2} = B_1^* e^{i\Delta\chi}; \;\; \mathbf{B}_2 = \mathbf{B}_1 e^{-i\Delta\chi}. \qquad (5)$$

This 2D easy-axis rotation theorem implies that dipole orientation maximizing a field component nulls the orthogonal component. In 3D, without loss of generality, coordinates can be oriented such that the point of interest is at the origin and the dipole is at $(0, 0, z_q)$. On-axis field $\mathbf{B}(0)$ is

$$(4\pi z_q^3/ql)\mathbf{B}(0) = (-\cos\chi, -\cos\psi, 2\cos\theta). \qquad (6)$$

In contrast to the 2D case, in 3D the magnitude $|B(0)|$ can vary by a factor of two, depending on the dipole orientation, being largest when the dipole is oriented in the direction of $\mathbf{r} - \mathbf{r}_q$:

$$(4\pi z_q^3/ql)|\mathbf{B}(0)| = \sqrt{3\cos^2\theta + 1}. \qquad (7)$$

Rotation of the dipole by $\Delta\phi_q$ in the x-y plane leaves B_z, $|B|$, and the sum $B_x^2 + B_y^2$ unchanged; individually, B_x and B_y are proportional to $\cos\phi_q$ and $\sin\phi_q$, respectively. Rotation by $\Delta\theta_q$ in any plane containing the z-axis leaves the ratio B_x/B_y unchanged; both B_x and B_y are proportional to $\sin\theta_q$, B_z is proportional to $\cos\theta_q$, and $|B| \propto \sqrt{3\cos^2\theta + 1}$. (See Fig. 1.)

D. Maximizing field components.

The formulas above are useful in determining the optimal orientation of magnetic moments in space to achieve a desired 3D field distribution. For example, in a 3D pure PM structure, using $|\hat{\eta}_q| = 1$, on-axis $B_y = f(\cos\psi, \cos\theta)$ and is given by:

$$\frac{4\pi|\mathbf{r}_q|^5}{ql} B_y(0,0,z) = 3x_q y_q \sqrt{1 - \cos^2\psi - \cos^2\theta}$$
$$+ (2y_q^2 - x_q^2 - \hat{z}_q^2)\cos\psi + 3y_q\hat{z}_q\cos\theta. \qquad (8)$$

It is maximized for $\hat{\eta}_q$ given by:

$$\begin{pmatrix} \cos\chi \\ \cos\psi \\ \cos\theta \end{pmatrix} = \left[(3x_q y_q)^2 + (2y_q^2 - x_q^2 - \hat{z}_q^2)^2 + (3y_q\hat{z}_q)^2\right]^{-1/2} \begin{pmatrix} 3x_q y_q \\ 2y_q^2 - x_q^2 - \hat{z}_q^2 \\ 3y_q\hat{z}_q \end{pmatrix}. \qquad (9)$$

Thus to maximize on-axis $B_y(0,0,z)$, easy-axis orientation of a dipole at, for example, location $z_q = z$ and

$$\left\{ \begin{array}{c} x_q = 0 \\ 2y_q^2 - x_q^2 = 0 \\ y_q = 0 \end{array} \right\} \text{ is } \hat{\eta}_q = \left\{ \begin{array}{c} (0,+1,0) \\ (+1,0,0) \\ (0,-1,0) \end{array} \right\}. \qquad (10)$$

At the other extreme, as $\hat{z}_q \longrightarrow \infty$ at any (x_q, y_q), the easy-axis orientation of a dipole that maximizes on-axis $B_y(0,0,z)$, is $\cos\psi = -1$.

Implications for pure PM ID design are tremendous. One can increase on-axis B by $\sim 20\%$ in the inherently 3D ALS EPU structure (λ = 5cm, gap=1.8cm) by rotating the PM easy-axis as one moves off-axis in x. (See Fig. 2.)

On-axis fields of conventional linear polarizing pure PM devices also can be increased dramatically by taking advantage of this third-dimension easy-axis directionality optimization. For example, for pure PM IDs of gap-period ratios of 0.5 and 0.07, 4 blocks-per-period, and block height $L = \lambda/2$, maximum B_y of a practical structure utilizing easy-axis orientation variation in the x-direction (with just three rows of blocks in x) increases by 5% and 40%, respectively, over their 2D counterparts. (See Fig. 3.) For large period devices, peak fields greater than 2.5T are achievable. Finer subdivsion of blocks can in principle more than double these percentage increases, but manufacturing and assembly becomes increasingly cumbersome. If fabrication simplicity is paramount, peak on-axis field can actually be increased beyond the 2D 'ideal' field

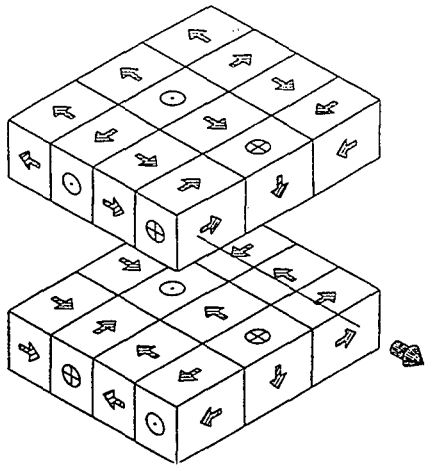

Fig. 3. Linear polarizing pure PM device with 3D field enhancement (one of many possible discretizations)

by merely truncating the PM blocks in the x-direction, since easy-axis orientation for maximizing peak on-axis B_y rotates through 180° as the x-coordinate of the dipole location varies within the interval $0 \leq x_q \leq \infty$.

Maximization of $B_x = f(\cos\psi, \cos\theta)$ is analogous:

$$\frac{4\pi|\mathbf{r}_q|^5}{ql} B_x(0,0,z) = (2x_q^2 - y_q^2 - \hat{z}_q^2)\sqrt{1-\cos^2\psi - \cos^2\theta}$$

$$+ 3x_q y_q \cos\psi + 3x_q \hat{z}_q \cos\theta. \qquad (11)$$

It is maximized for $\hat{\eta}_q$ given by:

$$\begin{pmatrix} \cos\chi \\ \cos\psi \\ \cos\theta \end{pmatrix} = [(2x_q^2 - y_q^2 - \hat{z}_q^2)^2 + (3x_q y_q)^2$$

$$+(3x_q\hat{z}_q)^2]^{-1/2} \begin{pmatrix} 2x_q^2 - y_q^2 - \hat{z}_q^2 \\ 3x_q y_q \\ 3x_q \hat{z}_q \end{pmatrix}. \qquad (12)$$

Thus to maximize on-axis $B_x(0,0,z)$, easy-axis orientation of a dipole at, for example, location $z_q = z$ and

$$\left\{ \begin{array}{c} x_q = 0 \\ 2x_q^2 - y_q^2 = 0 \\ y_q = 0 \end{array} \right\} \text{ is } \hat{\eta}_q = \left\{ \begin{array}{c} (-1,0,0) \\ (0,+1,0) \\ (+1,0,0) \end{array} \right\}. \qquad (13)$$

At the other extreme, as $\hat{z}_q \longrightarrow \infty$ at any (x_q, y_q), the easy-axis orientation of a dipole that maximizes on-axis $B_x(0,0,z)$, is $\cos\chi = -1$.

III. PM BLOCKS & PERIODIC STRUCTURES

The field $\mathbf{B}(x,y,z)$ due to a uniformly magnetized block can be determined from a charge sheet model over the block surface where $q = \mathbf{B}_r \cdot \mathbf{a}$, where $\mathbf{B}_r$ is the remanent field and $\mathbf{a}$ is the magnet's surface area. Referring to the PM block in Fig. 4, charge sheets may exist on any of the block's six faces, depending on the magnetization

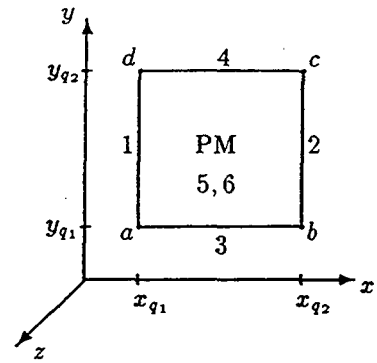

Fig. 4. PM block orientation and surfaces

orientation [5,6]. For a positive charge sheet on a single face:

$$\frac{4\pi}{B_r} B_u(x,y,z) = \int \frac{u - u_q}{|\mathbf{r} - \mathbf{r}_q|^3} da_q;$$

$$da_q = \left\{ \begin{array}{c} dx_q dy_q \\ dx_q dz_q \\ dy_q dz_q \end{array} \right\}; \ \mathbf{B}_r \parallel \left\{ \begin{array}{c} z \\ y \\ x \end{array} \right\}, \qquad (14)$$

where $u = x, y$, or z. Summing contributions from the individual faces for each PM block in a system yields the vector components of B at any arbitrary location(s), e.g. along the axis in a pure PM undulator. For blocks whose surfaces are not parallel to the cartesian axes, one can always perform coordinate transformations by axes rotation; thus the development herein is completely general. Two types of integrals must be evaluated: those where the charge sheet surface normal and the calculated field component are parallel ($\mathbf{a}_q \times \hat{\eta}_{B_u} = 0$) and when they are perpendicular ($\mathbf{a}_q \cdot \hat{\eta}_{B_u} = 0$). (See Appendix A for solution details using either varible substitutions or Green's theorem.) The first integral type is:

$$\frac{4\pi}{B_r} B_u(x,y,z) = \int\int \frac{-\hat{u}_q}{|\hat{\mathbf{r}}_q|^3} du_q dv_q \equiv O_1(u_q, v_q) = \quad (15)$$

$$\ln\left(\frac{[\hat{v}_{q_2} + |\hat{\mathbf{r}}_q(u_{q_2}, v_{q_2}, w_q)|][\hat{v}_{q_1} + |\hat{\mathbf{r}}_q(u_{q_1}, v_{q_1}, w_q)|]}{[\hat{v}_{q_2} + |\hat{\mathbf{r}}_q(u_{q_1}, v_{q_2}, w_q)|][\hat{v}_{q_1} + |\hat{\mathbf{r}}_q(u_{q_2}, v_{q_1}, w_q)|]} \right)$$

where u is the cartesian coordinate of the field component of interest, with u, v, w each being any one of the cartesian coordinates x, y, z. The normal to the charged block surface is parallel to the w axis and is defined by the region w_q=constant, $u_{q_1} \leq u_q \leq u_{q_2}$, and $v_{q_1} \leq v_q \leq v_{q_2}$. B_r is the surface charge sheet density and $|\hat{\mathbf{r}}_q(u_q, v_q, w_q)| \equiv \sqrt{(u_q - u)^2 + (v_q - v)^2 + (w_q - w)^2}$. The second integral type is:

$$\frac{4\pi}{B_r} B_u(x,y,z) = \int\int \frac{-\hat{u}_q}{|\hat{\mathbf{r}}_q|^3} dv_q dw_q \equiv O_2(u_q) = \quad (16)$$

$$\arctan\left(\frac{\hat{v}_{q_2}\hat{w}_{q_1}}{\hat{u}_q|\hat{\mathbf{r}}_q(u_q,v_{q_2},w_{q_1})|}\right)+\arctan\left(\frac{\hat{v}_{q_1}\hat{w}_{q_2}}{\hat{u}_q|\hat{\mathbf{r}}_q(u_q,v_{q_1},w_{q_2})|}\right)$$

$$-\arctan\left(\frac{\hat{v}_{q_1}\hat{w}_{q_1}}{\hat{u}_q|\hat{\mathbf{r}}_q(u_q,v_{q_1},w_{q_1})|}\right)-\arctan\left(\frac{\hat{v}_{q_2}\hat{w}_{q_2}}{\hat{u}_q|\hat{\mathbf{r}}_q(u_q,v_{q_2},w_{q_2})|}\right)$$

where u is the cartesian coordinate of the field component, the block surface defined by the region $u_q=$ const., $v_{q_1} \leq v_q \leq v_{q_2}$, and $w_{q_1} \leq w_q \leq w_{q_2}$ is normal to the v-w plane.

The field in a 3D structure of PM blocks, then, is

$$\frac{4\pi}{B_r}\begin{pmatrix} B_x(\mathbf{r}) \\ B_y(\mathbf{r}) \\ B_z(\mathbf{r}) \end{pmatrix} = \tag{17}$$

$$\begin{pmatrix} \sum_x O_2(x_q) & +\sum_y O_1(x_q,z_q) & +\sum_z O_1(x_q,y_q) \\ \sum_x O_1(y_q,z_q) & +\sum_y O_2(y_q) & +\sum_z O_1(y_q,x_q) \\ \sum_x O_1(z_q,y_q) & +\sum_y O_1(z_q,x_q) & +\sum_z O_2(z_q) \end{pmatrix},$$

where the summation Σ_x is over all charge sheet surfaces whose normal is parallel to the x axis, etc.

In the expression in Eq. (17), there is a singularity in the logarithm when $\hat{v}_q = -|\hat{\mathbf{r}}_q|$. These singularities occur in pairs and can be handled numerically taking the limit:

$$\lim_{\epsilon\longrightarrow 0} \ln\left(\frac{-a+\sqrt{a^2+\epsilon^2}}{-b+\sqrt{b^2+\epsilon^2}}\right) = \ln(b/a). \tag{18}$$

We have used the 3D optimization techniques of the previous section to design the ALS EPU shown in Figure 2, using the closed-form expressions of this section. Program CPU [7] allows input of multiple rows of periodic arrays of PM blocks with specified magnetization orientations to rapidly calculate fields anywhere in the gap region of the proposed ALS EPU.

Having two blocks in each quadrant enables another beneficial design feature, i.e., a thinner vacuum chamber wall, and thus smaller magnetic gap, over the portion of the chamber directly above/below the beam axis than otherwise possible with a uniform-in-x chamber thickness due to strength limits. This further increases the attainable peak on-axis field. Note that with the 3D field enhancement, field rolloff in x is rapid, thus complicating focusing effects.

IV. APPENDIX A: INTEGRAL DERIVATIONS

For the integral type of Eq. (17), using Green's theorem and noting that $B_x = -\partial V/\partial x = \partial V/\partial x_q$, gives

$$\frac{4\pi}{B_r}B_x(x,y,z) = \int\int \frac{-\hat{x}_q}{|\hat{\mathbf{r}}_q|^3}dx_q dy_q = \frac{4\pi}{B_r}\int\int \frac{\partial V}{\partial x_q}dx_q dy_q$$

$$= \frac{4\pi}{B_r}\oint V dy_q = \frac{4\pi}{B_r}\left(\int_b^c V dy_q + \int_d^a V dy_q\right), \tag{19}$$

where points a, b, c, d are shown in Fig. 4. Integral contributions along a-b and c-d are zero since y is constant along these line segments. Integrating Eq. (21) with V given by Eq. (1) yields Eq. (17). Alternatively,

$$\frac{4\pi}{B_r}B_x(x,y,z) = \int_{x_{q_1}}^{x_{q_2}} \left(\frac{\hat{x}_q}{\hat{x}_q^2+\hat{z}_q^2}\right)\left(\frac{\hat{y}_q}{|\hat{\mathbf{r}}_q|}\right)\Bigg|_{y_{q_1}}^{y_{q_2}} dx_q. \tag{20}$$

Now

$$\int\left(\frac{\hat{x}_q}{\hat{x}_q^2+c_1}\right)\left(\frac{1}{\sqrt{\hat{x}_q^2+c_2}}\right)dx_q = \int\frac{dp}{p^2-(c_2-c_1)}$$

$$= \frac{-1}{\sqrt{c_2-c_1}}\ln\left|\frac{\sqrt{c_2-c_1}+\sqrt{\hat{x}_q^2+c_2}}{i\sqrt{\hat{x}_q^2+c_1}}\right|, \tag{21}$$

where $p \equiv \sqrt{\hat{x}_q^2+c_2}$, $c_1 = \hat{z}_q^2$, and $c_2 - c_1 = \hat{y}_q^2$. Making the substitutions again yields Eq. (17).

Similarly, for the integral type of Eq. (18),

$$\frac{4\pi}{B_r}B_x(x,y,z) = \int_{z_{q_1}}^{z_{q_2}} \left(\frac{\hat{x}_q}{\hat{x}_q^2+\hat{z}_q^2}\right)\left(\frac{\hat{y}_q}{|\hat{\mathbf{r}}_q|}\right)\Bigg|_{y_{q_1}}^{y_{q_2}} dz_q. \tag{22}$$

Now

$$\int\left(\frac{1}{\hat{z}_q^2+c_1}\right)\left(\frac{1}{\sqrt{\hat{z}_q^2+c_2}}\right)dz_q = \int\frac{dp}{p^2(c_2-c_1)+c_1}$$

$$= \frac{1}{\sqrt{c_1}\sqrt{c_2-c_1}}\arctan\left(p\sqrt{\frac{c_2}{c_1}-1}\right), \tag{23}$$

where $p \equiv \hat{z}_q/\sqrt{\hat{z}_q^2+c_2}$, $c_1 = \hat{x}_q^2$, and $c_2 - c_1 = \hat{y}_q^2$. Making the substitutions yields Eq. (18).

ACKNOWLEDGMENT

We are happy to thank Klaus Halbach for teaching us the magnetics fundamentals on which this work is based.

REFERENCES

[1] K. Halbach, "Design of permanent multipole magnets with oriented rare earth cobalt material", *Nucl. Instr. Meth.* vol. 169, p. 1, 1980.

[2] K. Halbach, "Physical and optical properties of rare earth cobalt magnets", *Nucl. Instr. Meth.* vol. 187, p. 109, 1981.

[3] S. Sasaki, "Design of a new type of planar undulator for generating variably polarized radiation", *Nucl. Instr. Meth.* vol. A331, p. 763, 1993.

[4] S. Sasaki, "Analysis for a planar variably polarizing undulator", *Proc. 8th Nat. Conf. on Synch. Rad. Instr.* Gaithersburg, MD, 1993.

[5] K. Halbach, "Insertion device design", LBL Report V8811-1.1-16, 1989.

[6] R.D. Schlueter, "Field errors in hybrid insertion devices", *Halbach Symposium on Magnet Technology* vol. 1, LBL Report 36839, p. 55, 1995.

[7] R.D. Schlueter, *Code CPU*, Lawrence Berkeley Lab., 1995.

LAWRENCE BERKELEY LABORATORY
UNIVERSITY OF CALIFORNIA
TECHNICAL AND ELECTRONIC
INFORMATION DEPARTMENT
BERKELEY, CALIFORNIA 94720